Available online at www.sciencedirect.com
ScienceDirect
Journal of Sound and Vibration 313 (2008) 738–759
JOURNAL OF SOUND AND VIBRATION
www.elsevier.com/locate/jsvi

Modes coupling due to nonhomogeneously shaped walls in duct acoustics

Catherine Potel*, Michel Bruneau

Laboratoire d'Acoustique de l'Université du Maine (LAUM), UMR CNRS 6613, Université du Maine, Avenue Olivier Messiaen, 72 085 Le Mans Cedex 9, France

Received 26 June 2007; received in revised form 2 December 2007; accepted 5 December 2007
Available online 7 January 2008

Abstract

The acoustic pressure field inside finite or infinite, fluid-filled waveguides with surfaces having distributed small deviations (corrugation, roughness, facade irregularities in streets and so on) from the regular shape (smooth surface) is studied, using an approach called shape profile model. In this approach, the acoustic field is obtained from the coupling between Neumann modes of the regularly shaped surface that bounds outwardly the perturbed surface of the waveguide (i.e. on outer side of the perturbed surface). The effect of the rough boundaries on the acoustic field is modelled by an operator acting on the acoustic pressure, which takes into account both the depth and the slopes of the profile. Two coupling mechanisms are identified, namely the "bulk" or "global" modal coupling and the "boundary" or "local" modal coupling. This model departs from those available until now because it does not make use of the so-called multimodal approach: it lies on the integral formulation in the frame of a modal approach using a unique set of eigenfunctions, in order to obtain the pressure field inside the wave guide as a coupling between modes.

1. Introduction

The literature abounds with many papers in which topics involving acoustic fields within both closed region and finite or infinite waveguides are of principal focus. Nowadays, among others, there exists an understanding that acoustic modes coupling occurs in fluid-filled, irregular-shaped cavities, which provides methodology for predicting acoustical properties of enclosed sound fields [1–10]. The mathematical methods used rely on standard integral formulation and modal analysis, and the physical mechanisms, which have been investigated until now are those related to the nature of the modes coupling in the frequency domain.

Regarding the analytical solutions for describing the acoustic coupling in fluid-filled, irregular-shaped waveguides, when these irregularities are distributed along the walls of the guides, papers are concerned with effect of roughness surfaces, corrugated walls, surfaces involving periodicities, metal-strip grating, and so on. Analytical, numerical and experimental methods are involved in these studies [11–29]. Most of the analytical works deal primarily, among others, with (i) the description of the roughness and its effects on plane waves,

*Corresponding author. Tel.: +33 2 43 83 36 17; fax: +33 2 43 83 35 20.
E-mail addresses: Catherine.Potel@univ-lemans.fr (C. Potel), Michel.Bruneau@univ-lemans.fr (M. Bruneau).

0022-460X/$ - see front matter © 2007 Elsevier Ltd. All rights reserved.
doi:10.1016/j.jsv.2007.12.001

Nomenclature

$\hat{a}_\mu$	amplitude of the mode μ in the modal expansion of the acoustic pressure $\hat{p}(\mathbf{r};t)$
$\hat{A}_\mu$, $\tilde{\hat{A}}_\mu$	amplitude of the mode μ in the modal expansion of the acoustic pressure for a monochromatic source, function of x_1, x_2 or of ξ_1, see Eqs. (20a) and (26d)
$\hat{A}_m^{[n]}$	nth-order perturbation expansion for $\hat{A}_m$
$\hat{A}_m^{(n)}$	nth-order correction term, see Eq. (39)
$B_{\mu m}$	see Eq. (13a): $B_{\mu m} = \lvert\beta_{\mu m}\rvert\eta_0(x_1,x_2) + \beta_{\mu m}\eta_d(x_1,x_2)$
c_0	adiabatic speed of sound
C_m^0	amplitude of an incoming wave, created by an acoustic source of strength $\hat{S}_m$
d	thickness of the inner waveguide surrounded by the corrugated waveguide considered
$D_\parallel$	domain $x_1 \in [0,+\infty[$, $x_2 \in]-\infty,+\infty[$ and $0 \leqslant x_3 \leqslant d$
f	frequency
$\hat{f}(\mathbf{r};t)$	source function
$\hat{G}_m$	coefficient of the expansion of the modal Green function for the quantum number m
H	$H = H_0 + H_d$
H_0, H_d	depths of the small shape deviations at $x_3 = 0$ and δ
k_0	wavenumber $k_0 = \omega/c_0$
k_m	eigenvalue such that $k_m = m\pi/\delta$, $m \in \mathbb{N}$
$k_{x_1 m}$, $k_{\xi_1 m}$	wavenumbers such that $k_{\xi_1 m}^2 = k_{x_1 m}^2 = k_0^2 - k_m^2$, see Eqs. (20d) and (26b)
ℓ	total length of the corrugation
m	quantum number of the mode considered
$\mathbf{n}_0$, $\mathbf{n}_d$	local unit vectors normal to the real surface of the waveguide at the points $x_3 = H_0$ and $x_3 = \delta - H_d$, and pointing outside the fluid
N	number of teeth in a profile
$N_{\mu m}$	see Eq. (10), $N_{\mu m}(x_1,x_2) = \int_{H_0}^{\delta - H_d} \psi_m(x_3)\psi_\mu(x_3)\,\mathrm{d}x_3$
$O(\mathbf{r};t)$	operator $O(\mathbf{r};t) = \pm\{(\partial_{x_1}H)\partial_{x_1} + (\partial_{x_2}H)\partial_{x_2}\}$
$\hat{p}(\mathbf{r};t)$	acoustic pressure
$\hat{Q}_m$	strength of the source $\hat{S}_m$ located at $x_1 = 0$ and $x_2 = 0$, see Eq. (38)
$\mathbf{r}$	position vector with components x_1, x_2 and x_3
$\mathbf{r}_\parallel$	vector with components x_1 and x_2
$\hat{s}_m$	inner product of the source function and the eigenfunction ψ_m
$\hat{S}_m$, $\tilde{\hat{S}}_m$	inner product of the monochromatic source function and the eigenfunction ψ_m, function of x_1, x_2 or of ξ_1
t	time
x_1, x_2, x_3	coordinates, x_3 being the transverse coordinate
z_0, z_d	total depths of the small shape deviations, respectively, on the walls $x_3 = 0$ and δ
$Z(x_1)$	integral of $\eta(x_1)$ from 0 to x_1
$\alpha_{\mu m}^{(j)}$	operator, see Eq. (18b)
$\beta_{\mu m}$	see Eq. (13b), $\beta_{\mu m} = (-1)^{m+\mu}\sqrt{(2-\delta_{m0})(2-\delta_{\mu 0})}$
$\widehat{\gamma}_{\mu m}$	coupling operator, see Eq. (18a)
δ	thickness of the waveguide which encloses the corrugated waveguide considered. $\delta = d + z_0 + z_d$
δ_{mn}	Kronecker tensor
$\delta(x)$	Dirac delta function
$\Delta_\parallel$	Laplacian for x_1 and x_2: $\Delta_\parallel = \partial_{x_1 x_1}^2 + \partial_{x_2 x_2}^2$
η, $\tilde{\eta}$	$\eta = \eta_0 + \eta_d$, function of x_1, x_2 or of ξ_1
η_0, η_d	ratio of the depths H_0, H_d to the thickness δ: $\eta_0 = H_0/\delta$, $\eta_d = H_d/\delta$
λ	acoustic wavelength, $\lambda = 2\pi/k_0$
$\lambda_{x_1 m}$	acoustic wavelength along the x_1-axis (or ξ_1-axis), $\lambda_{x_1 m} = 2\pi/k_{x_1 m}$
Λ	length of the spatial period of a periodic profile
μ	quantum number of a mode
$\xi_1(x_1)$	new variable, function of x_1, see Eqs. (23) and (24a)
$\psi_m(x_3)$	orthogonal and normalised eigenfunctions
ω	angular frequency
ϖ_m	see Eq. (26a)
$\hat{}$	complex quantity
$\sim$	quantity function of ξ_1 and no more of x_1

(ii) the description of plane-wave scattering states and their consequences, (iii) the method of multiple scales to analyse the modal coupling, (iv) the multimodal analysis; in all cases, the acoustic field is investigated both in fluid and solid media. But the analytic procedure whereby such perturbed acoustic field in fluid medium can be expressed as a sum over the unique set of the eigenmodes of the regular-shaped waveguide (not over series of

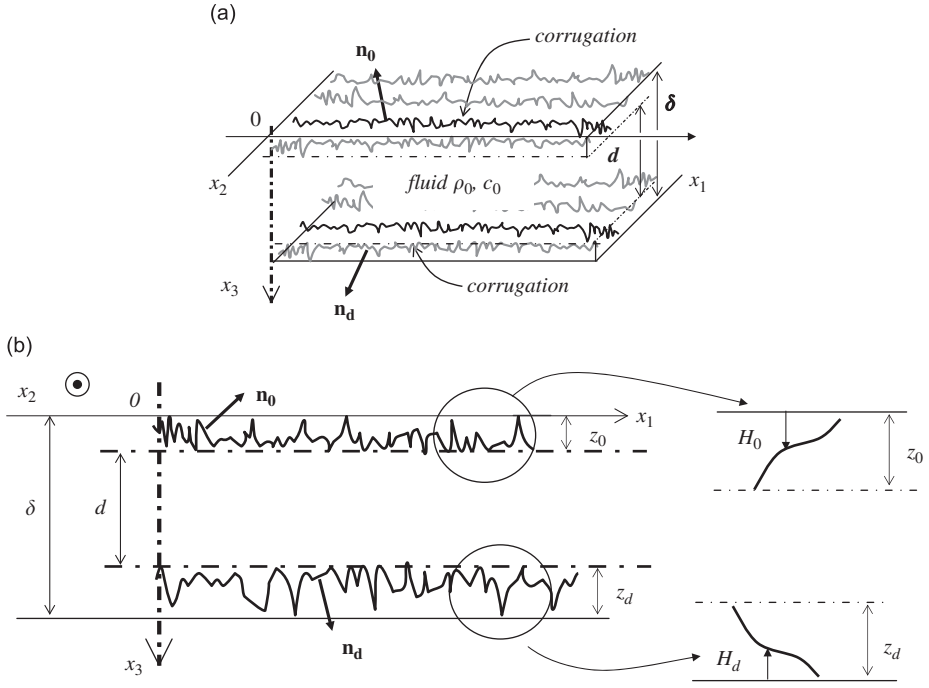

Fig. 1. Fluid plate between two perturbed boundary surfaces.

as many sets of eigenfunctions as it is necessary to follow the shape of the profile of the real nonhomogeneously shaped waveguide), this sum accounting for a continuously distributed modes coupling (along a distributed slight geometrical perturbation) through a method relying on the Green's theorem and the associated integral formulation, provides situations not considered so far to our knowledge.

Therefore, in the present paper, the acoustic wave propagation in infinite waveguides with surfaces having small deviations from the regular shape is dealt with (see an example of such waveguide sketches in Fig. 1a, showing the two-dimensional (2D) corrugation lying on the planes set at $x_3 = 0$ and d, the propagation taking place in the fluid-filled waveguide between these planes). The study is extensively analytical and relies on standard integral formulation to describe the nonlocal coupling between modes of a guide with regularly shaped surface (smooth surface) that bounds the perturbed surface, the nonhomogeneously shaped surface being finite in extent. The nonlocal effect of the surface perturbation is described by the integral formulation, introduced through the Green's theorem; the modal coupling created by the surface perturbation is emphasised by the modal analysis, establishing an explicit means which can highlight the properties of the acoustic field in many situations (as indicated below). Despite the apparent simplicity of the model, the analytical results can be complicated functions of the parameters, which govern the behaviour of the acoustic field.

In the approach used, called "shape profile model", the boundaries are modelled as geometrically perturbed surfaces, assuming Neumann (acoustically hard surface) conditions. The acoustic field is obtained from the coupling between Neumann modes of the regularly shaped surface that bounds outwardly (i.e. on outer side of the perturbed surface) the perturbed surface of the waveguide. Two coupling mechanisms are identified, namely the "bulk" or "global" modal coupling and the "boundary" or "local" modal coupling [7]. The former is related to the coupling of modes throughout the section of the guide (arising from the nonorthogonality of the modes in the perturbed lateral dimensions of the guide due to the depth of the surface perturbation), while the latter is related to the coupling through the slope and the depth of the surface perturbation. The behaviour of the acoustic pressure field is determined by these two mechanisms when propagating along the axis of the waveguide. The continuously distributed modes coupling along the distributed slight geometrical perturbation is accounted for in using method relying on integral formulation and modal analysis. Several applications to

guided waves propagating between two parallel walls, having regularly or randomly distributed shape perturbations, are presented, showing results expected (or known).

The main purpose of the paper is to contribute at providing an understanding of the physical phenomena involved and a tractable model to calculate the mode coupling due to small shape deviation of the wall of the waveguides (see Fig. 1a, the motion of the fluid being assumed to be inviscid and irrotational). This model departs from those available until now because it does not make use of the so-called multimodal approach: it lies on the integral formulation in the frame of a modal approach using a unique set of eigenfunctions, in order to obtain the pressure field inside the wave guide as a coupling between modes. Several examples are discussed to highlight the main properties of the acoustic fields considered. It is worth noting that the analytical formalism is applicable not only to infinite, semi-infinite or finite waveguide of any global shape (depending on the Green's function chosen in the integral formulation) as long as the nonperturbed eigenmodes are known, but also to closed cavities having small or large shape deviations [1–9].

2. The shape profile model

The waveguide is assumed to be bounded by two parallel plates having 2D shape perturbations (three-dimensional problem, Fig. 1a). The fluid layer (sometimes called fluid plate), with regularly shaped surfaces $x_3 = 0$ and δ, which encloses the corrugated waveguide considered, is characterized by its thickness δ, the inner plate surrounded by the corrugated waveguide is characterized by its thickness d; then, denoting the total depths of the small shape deviations z_0 and z_d, respectively, on the walls $x_3 = 0$ and δ, gives $\delta = d + z_0 + z_d$ (Fig. 1b). The depth of the small shape deviations, i.e. the distance between the outer plates with regular shape (thickness δ) and the shape perturbed walls are, respectively, denoted $H_0(x_1, x_2)$ and $H_d(x_1, x_2)$ at $x_3 = 0$ and $x_3 = \delta$, or $H(x_1, x_2, x_3 = 0, \delta)$. Thus, the coordinates of the real boundaries of the shape perturbed plates are given by

$$x_3 = H_0(x_1, x_2) \quad \text{and} \quad x_3 = \delta - H_d(x_1, x_2). \tag{1}$$

Since the coordinates x_1, x_2 and x_3 are dependent on each other on the perturbed surface, the acoustic field cannot be analytically resolved into independent components in the x_1, x_2 and x_3 directions. As a result, the acoustic pressure field in the waveguide with surfaces having distributed small deviations can be expressed as the eigenfunction expansion where the orthogonal eigenfunctions are solution of the Neumann boundary problem in the regularly shaped waveguide of which surfaces bound outwardly the perturbed waveguide. Therefore, rigid-walled modes of the bounding regular-shaped cavity (which encloses the waveguide with perturbed surface) are used to express the mode coupling which occurs in the region bounded by the perturbed surface.

2.1. The boundary conditions

The boundary conditions satisfied by the acoustic field on the perturbed surface of the waveguide are given by the requirement that its normal derivative on the surface vanishes at every point of the boundary. Denoting $\mathbf{n}_0$ the local unit vector normal to the real surface of the waveguide at the point $x_3 = H_0(x_1, x_2)$ and pointing outside the fluid, the normal derivative defines as $\partial_{\mathbf{n}_0} = \mathbf{n}_0 \cdot \nabla$ takes the classical form

$$\partial_{\mathbf{n}_0} = \mathbf{n}_0 \cdot \nabla = -\frac{1}{N_0}[-(\partial_{x_1} H_0)\partial_{x_1} - (\partial_{x_2} H_0)\partial_{x_2} + \partial_{x_3}] \tag{2a}$$

with

$$N_0 = \sqrt{1 + (\partial_{x_1} H_0)^2 + (\partial_{x_2} H_0)^2}. \tag{2b}$$

In the same manner, denoting $\mathbf{n}_d$ the local unit vector normal to the real surface of the waveguide at the point $x_3 = \delta - H_d(x_1, x_2)$ and pointing outside the fluid, the normal derivative defines as $\partial_{\mathbf{n}_d} = \mathbf{n}_d \cdot \nabla$ takes

the classical form

$$\partial \mathbf{n}_d = \mathbf{n}_d \cdot \nabla = \frac{1}{N_d}[(\partial_{x_1} H_d)\partial_{x_1} + (\partial_{x_2} H_d)\partial_{x_2} + \partial_{x_3}] \tag{3a}$$

with

$$N_d = \sqrt{1 + (\partial_{x_1} H_d)^2 + (\partial_{x_2} H_d)^2}. \tag{3b}$$

Thus, the Neumann boundary conditions can be written in the form

$$\partial \mathbf{n}_0 \hat{p} = 0$$

$$\text{i.e.} \quad \partial_{x_3} \hat{p} = [(\partial_{x_1} H_0)\partial_{x_1} + (\partial_{x_2} H_0)\partial_{x_2}]\hat{p} \tag{4}$$

and $\partial \mathbf{n}_d \hat{p} = 0$

$$\text{i.e.} \quad \partial_{x_3} \hat{p} = -[(\partial_{x_1} H_d)\partial_{x_1} + (\partial_{x_2} H_d)\partial_{x_2}]\hat{p}. \tag{5}$$

Generally speaking, these Neumann conditions (4) and (5) can be written as follows:

$$\partial_{x_3} \hat{p} = O(\mathbf{r}; t)\hat{p}, x_3 = H_0(x_1, x_2) \quad \text{and} \quad x_3 = \delta - H_d(x_1, x_2), \tag{6a}$$

where the operator $O(\mathbf{r}; t)$ is defined as

$$O(\mathbf{r}; t) = \pm\{(\partial_{x_1} H)\partial_{x_1} + (\partial_{x_2} H)\partial_{x_2}\} \tag{6b}$$

with the sign "+" for $x_3 = H_0(x_1, x_2)$ at the upper interface and the sign "−" for $x_3 = \delta - H_d(x_1, x_2)$ at the lower interface.

2.2. The fundamental problem

In the problem addressed here, it is assumed that sources which are set at the input of the considered domain (at the entrance $x_1 = 0$ of the corrugated waveguide) are such as they create an acoustic field with a given profile in the x_3-direction, or are incident propagating wave coming from $x_1 \to -\infty$. Therefore, the acoustic pressure denoted $\hat{p}(\mathbf{r}; t)$ is governed by the set of equations including the propagation equation and the boundary conditions, which is written as

$$\left(\Delta_\parallel + \partial^2_{x_3 x_3} - \frac{1}{c_0^2}\partial^2_{tt}\right)\hat{p}(\mathbf{r}; t) = -\hat{f}(\mathbf{r}; t), \; H_0 \leqslant x_3 \leqslant \delta - H_d, \; \forall \mathbf{r}_\parallel \in D_\parallel, \tag{7a}$$

$$\partial_{x_3} \hat{p}(\mathbf{r}; t) = O(\mathbf{r}; t)\hat{p}(\mathbf{r}; t), \; x_3 = H_0(x_1, x_2) \quad \text{and} \quad x_3 = \delta - H_d(x_1, x_2), \; \forall \mathbf{r}_\parallel \in D_\parallel, \tag{7b}$$

$$\text{Sommerfeld condition when} \quad D_\parallel \text{ is infinite}, \tag{7c}$$

where $\Delta_\parallel = \partial^2_{x_1 x_1} + \partial^2_{x_2 x_2}$, ∂^2_{tt} and ∂_{x_i} stand, respectively, for $\partial^2/\partial t^2$ and $\partial/\partial x_i$, the source function $\hat{f}(\mathbf{r}; t)$ being assumed to generate an incoming wave at the entrance of the domain of interest $D_\parallel$ ($D_\parallel$ is the domain $x_1 \in [0, +\infty[$, $x_2 \in]-\infty, +\infty[$), x_1 and x_2 being the two components of the vector $\mathbf{r}_\parallel$, and x_1, x_2 and x_3 the components of the vector $\mathbf{r}$. The operator $O(\mathbf{r},t)$, which represents the effect of the shape perturbations of the boundaries (Eq. (6b)) is here a complicated operator acting on the spatial coordinates.

2.3. The eigenvalue problem

The solution can readily be expressed in terms of one-dimensional eigenmodes of the three-dimensional waveguide bounded by the regularly shaped, parallel, and plane surfaces set at $x_3 = 0$ and δ on the outer side of the perturbed surfaces (Fig. 1b), using the modal wave functions that are solutions of the homogeneous Helmholtz equation subject to Neumann boundary conditions, namely

$$(\partial^2_{x_3 x_3} + k_m^2)\psi_m(x_3) = 0, \quad 0 \leqslant x_3 \leqslant \delta, \tag{8a}$$

$$\partial_{x_3}\psi_m(x_3) = 0, \quad x_3 = 0 \quad \text{and} \quad x_3 = \delta, \tag{8b}$$

where the eigenvalues k_m and the eigenfunctions (orthogonal and normalised) ψ_m are given, respectively, by

$$k_m = m\pi/\delta, \quad m \in \mathbb{N} \tag{9a}$$

and

$$\psi_m(x_3) = \sqrt{(2-\delta_{m0})/\delta}\,\cos(k_m x_3), \tag{9b}$$

δ_{m0} being the Kronecker tensor.

The construction of solutions given below in terms of modal wavefunctions makes use of the following integral (over the range $H_0 \leqslant x_3 \leqslant \delta - H_d$):

$$N_{\mu m}(x_1, x_2) = \int_{H_0}^{\delta - H_d} \psi_m(x_3)\psi_\mu(x_3)\,\mathrm{d}x_3, \tag{10}$$

which is given, to the first-order of the small dimensionless quantities (see details in Appendix A):

$$\eta_0(x_1, x_2) = H_0(x_1, x_2)/\delta \tag{11a}$$

and

$$\eta_d(x_1, x_2) = H_d(x_1, x_2)/\delta \tag{11b}$$

by

$$N_{\mu m}(x_1, x_2) = \delta_{\mu m} - B_{\mu m} \tag{12}$$

with

$$B_{\mu m} = |\beta_{\mu m}|\eta_0(x_1, x_2) + \beta_{\mu m}\eta_d(x_1, x_2). \tag{13a}$$

$\beta_{\mu m}$ being given by

$$\beta_{\mu m} = (-1)^{m+\mu}\sqrt{(2-\delta_{m0})(2-\delta_{\mu 0})}. \tag{13b}$$

It is noteworthy that $N_{\mu m}(x_1, x_2)$ is not a scalar product of eigenfunctions, solutions of the set of Eq. (8), because the integration lies on the interval $[H_0;\ \delta - H_d]$ and not on the interval $[0;\delta]$.

2.4. Modal formulation

Expanding the pressure field on the eigenfunctions (9), namely,

$$\hat{p}(x_1, x_2, x_3; t) = \sum_\mu \hat{a}_\mu(x_1, x_2; t)\psi_\mu(x_3) \tag{14}$$

multiplying Eq. (7a) by the eigenfunction $\psi_m(x_3)$, and integrating over the range $H_0 \leqslant x_3 \leqslant \delta - H_d$:

$$\begin{aligned}\int_{H_0}^{\delta - H_d} \psi_m(x_3)\left(\Delta_\parallel + \partial^2_{x_3 x_3} - \frac{1}{c_0^2}\partial^2_{tt}\right)\hat{p}(x_1, x_2, x_3; t)\,\mathrm{d}x_3 \\ = -\int_{H_0}^{\delta - H_d} \psi_m(x_3)\hat{f}(x_1, x_2, x_3; t)\,\mathrm{d}x_3,\end{aligned} \tag{15}$$

solution of the posed problem for the acoustic pressure field is subsequently achieved with the help of Green's integral theorem which states

$$\sum_\mu N_{\mu m}(x_1, x_2)\left(\Delta_\parallel - k_m^2 - \frac{1}{c_0^2}\partial^2_{tt}\right)\hat{a}_\mu(x_1, x_2; t) = -\hat{s}_m(x_1, x_2; t) - \sum_\mu \hat{\gamma}_{\mu m}(x_1, x_2)\hat{a}_\mu(x_1, x_2; t), \tag{16}$$

where

$$\hat{s}_m(x_1, x_2; t) = \int_{H_0}^{\delta - H_d} \psi_m(x_3) \hat{f}(x_1, x_2, x_3; t)\, \mathrm{d}x_3, \tag{17}$$

$$\hat{\gamma}_{\mu m}(x_1, x_2) = -\{\alpha^{(1)}_{\mu m} \partial_{x_1} + \alpha^{(2)}_{\mu m} \partial_{x_2} + k_m^2 B_{\mu m}\} \tag{18a}$$

with

$$\alpha^{(j)}_{\mu m}(x_1, x_2) = |\beta_{\mu m}| \partial_{x_j}[\eta_0(x_1, x_2)] + \beta_{\mu m} \partial_{x_j}[\eta_d(x_1, x_2)] \tag{18b}$$

$\beta_{\mu m}$ and $B_{\mu m}$ being given, respectively, by Eqs. (13b) and (13a).

Eq. (16) indicates what are the mechanisms involved in the modes coupling. Two coupling mechanisms can be identified, namely the "bulk" or "global" modal coupling and the "boundary" or "local" modal coupling [7]. The former, expressed in the left-hand side of Eq. (16) by the term $N_{\mu m}$, is related to the coupling of modes throughout the section of the guide (arising from the nonorthogonality of the modes in the perturbed lateral dimensions of the guide due to the depth of the surface perturbation), while the latter, expressed in the right-hand side of Eq. (16) by the term $\widehat{\gamma}_{\mu m}$, is related to the coupling through the slope and the depth of the surface perturbation itself. The behaviour of the acoustic pressure field is determined by these two mechanisms when propagating along the axis of the waveguide, the continuously distributed modes coupling along the distributed slight geometrical perturbation being accounted for in using method relying on integral formulation.

Taking expression (12) for $N_{mm}(x_1, x_2)$ into Eq. (16), gives, for a harmonic motion (angular frequency $\omega = k_0 c_0$):

$$\begin{aligned}(\Delta_\parallel + k^2_{x_1 m})\hat{A}_m(x_1, x_2) = &-\hat{S}_m(x_1, x_2) + \beta_{mm}\eta(x_1, x_2)(\Delta_\parallel + k^2_{x_1 m})\hat{A}_m(x_1, x_2) \\ &- \sum_{\mu \neq m} N_{\mu m}(x_1, x_2)(\Delta_\parallel + k^2_{x_1 m})\hat{A}_\mu(x_1, x_2) - \sum_{\mu} \hat{\gamma}_{\mu m}(x_1, x_2)\hat{A}_\mu(x_1, x_2),\end{aligned} \tag{19}$$

where

$$\hat{a}_m(x_1, x_2; t) = \hat{A}_m(x_1, x_2) \exp(+\mathrm{i}\omega t), \tag{20a}$$

$$\hat{s}_m(x_1, x_2; t) = \hat{S}_m(x_1, x_2) \exp(+\mathrm{i}\omega t), \tag{20b}$$

$$\eta(x_1, x_2) = \eta_0(x_1, x_2) + \eta_d(x_1, x_2) \tag{20c}$$

with

$$k^2_{x_1 m} = k_0^2 - k_m^2. \tag{20d}$$

The complete resolution of Eq. (19), using integral formulation and inter-modal coupling, is given in Section 4. In order to highlight the basic phenomena, an approximate qualitative solution, called "monomode approach", is presented in Section 3.

3. Approximate monomode approach: highlighting of basic phenomena

This first approach is just a qualitative model in order to provide (in particular) a very simple analytical solution, which highlights the basic scattering phenomena on the irregularities.

3.1. Monomode, one-dimensional propagation equation

In this section, the mode labelled m is assumed to be the only one which is created by an acoustic source of strength $\hat{S}_m$ ($\hat{S}_{\mu \neq m} = 0$) set at $x_1 < 0$ i.e. on the left of the input of the corrugation (Fig. 1), the amplitude of this incoming wave at $x_1 = 0$ being denoted C_m^0. This mode propagates inside a waveguide bounded by surfaces with one-dimensional corrugation (2D problem, $x_3 \in [H_0, \delta - H_d]$). Therefore, when the

cross-coupling between any mode μ and the mode m ($\mu \neq m$) is neglected, Eq. (19) gives, outside the sources,

$$[1 - \beta_{mm}\eta(x_1)](\Delta_{\parallel} + k_{x_1 m}^2)\hat{A}_m(x_1) = -\hat{\gamma}_{mm}(x_1)\hat{A}_m(x_1). \tag{21}$$

Then, reporting expression (18) for the term $\hat{\gamma}_{mm}(x_1)$, Eq. (21), truncated to include only the first-order perturbation expansion with respect to the dimensionless small quantity $\eta(x_1)$, becomes

$$\{\Delta_{\parallel} - \beta_{mm}\partial_{x_1}[\eta(x_1)]\partial_{x_1} + k_{x_1 m}^2 - k_m^2\beta_{mm}\eta(x_1)\}\hat{A}_m(x_1) = 0. \tag{22}$$

It is convenient to change the variable x_1 as follows:

$$\xi_1 = \int_0^{x_1} \exp\left[\int_0^{x_1'} \beta_{mm}\partial_{x_1''}[\eta(x_1'')]\,\mathrm{d}x_1''\right]\mathrm{d}x_1' \tag{23a}$$

i.e.

$$\xi_1 = \int_0^{x_1} \exp[\beta_{mm}\eta(x_1')]\,\mathrm{d}x_1' \tag{23b}$$

because $\eta(0) = 0$. Expanding the exponential function to the first-order of the small parameter $\eta(x_1')$, the change of variable reduces to

$$\xi_1 \approx x_1 + \beta_{mm}Z(x_1), \tag{24a}$$

where

$$Z(x_1) = \int_0^{x_1} \eta(x_1')\,\mathrm{d}x_1' \tag{24b}$$

and then, Eq. (22) takes the form

$$(\partial_{\xi_1\xi_1}^2 + k_{\xi_1 m}^2[1 + \varpi_m\tilde{\eta}(\xi_1)])\tilde{\hat{A}}_m(\xi_1) = 0, \tag{25}$$

where

$$\varpi_m = -(2 - \delta_{m0})(2 + k_m^2/k_{\xi_1 m}^2), \tag{26a}$$

$$k_{\xi_1 m}^2 = k_{x_1 m}^2 = k_0^2 - k_m^2, \tag{26b}$$

$$\tilde{\eta}(\xi_1) = \eta[\xi_1(x_1)], \tag{26c}$$

$$\tilde{\hat{A}}_m(\xi_1) = \hat{A}_m[\xi_1(x_1)]. \tag{26d}$$

In some circumstances, namely when considering interior problems (i.e. finite waveguides or cavities), losses must be taken into account when the frequency is monitored to make the field resonant (here when $k_{\xi_1 m} = 0$) because the solutions must behave accurately, and therefore it is consequent to express adequately the dissipation processes, namely the viscous and thermal effects in the boundary layers near the rigid walls as well as a priori in the bulk of the cavity. But, in practice, such resonant field will not be used, because the only propagative modes would be relevant for the characterisation of the roughness. Therefore, subsequently, it is assumed that $k_{\xi_1 m}$ is a finite positive quantity (even if it is not necessary in this section because, in fact, this factor does not appear in the denominator of Eq. (25)).

3.2. Approximate solution

The analytical expression of the amplitude $\tilde{\hat{A}}_m(\xi_1)$ of the approximate pressure field, solution of Eq. (25), is truncated to include only the first-order expansion with respect to the small quantity $\tilde{\eta}(\xi_1)$. This approximate solution, denoted $\tilde{\hat{A}}_m^{[1]}(\xi_1)$, can be written as

$$\tilde{\hat{A}}_m^{[1]}(\xi_1) = \tilde{\hat{A}}_m^{(0)}(\xi_1) + \tilde{\hat{A}}_m^{(1)}(\xi_1) = \tilde{\hat{A}}_m^{(0)}(\xi_1)[1 + \varepsilon(\xi_1)], \tag{27}$$

where the function $\tilde{\tilde{A}}_m^{(0)}(\xi_1)$, which can be considered as the zero-order expansion with respect to $\tilde{\eta}(\xi_1)$ and thus is solution of the following equation:

$$(\partial^2_{\xi_1\xi_1} + k^2_{\xi_1 m})\tilde{\tilde{A}}_m^{(0)}(\xi_1) = 0 \tag{28}$$

takes the form

$$\tilde{\tilde{A}}_m^{(0)}(\xi_1) = C_m^0 \exp(-\mathrm{i}k_{\xi_1 m}\xi_1), \tag{29}$$

C_m^0 being here a constant given by the amplitude of the incoming wave at $x_1 = \xi_1 = 0$.

Then, the first-order term which appears in expression (27)

$$\tilde{\tilde{A}}_m^{(1)}(\xi_1) = \tilde{\tilde{A}}_m^{(0)}(\xi_1)\varepsilon(\xi_1) \tag{30}$$

is the solution of the ordinary differential equation

$$\frac{\mathrm{d}}{\mathrm{d}\xi_1}\left(\frac{\mathrm{d}}{\mathrm{d}\xi_1} - 2\mathrm{i}k_{\xi_1 m}\right)\varepsilon(\xi_1) = -k^2_{\xi_1 m}\varpi_m\tilde{\eta}(\xi_1) \tag{31}$$

leading to, for a wave propagating in the direction of the ξ_1-axis,

$$\left(\frac{\mathrm{d}}{\mathrm{d}\xi_1} - 2\mathrm{i}k_{\xi_1 m}\right)\varepsilon(\xi_1) = F(\xi_1), \tag{32}$$

where

$$F(\xi_1) = -k^2_{x_1 m}\varpi_m\tilde{Z}(\xi_1) + C_1 \tag{33a}$$

with

$$\tilde{Z}(\xi_1) = \int_0^{\xi_1}\tilde{\eta}(\xi)\,\mathrm{d}\xi \tag{33b}$$

C_1 being an arbitrary constant.

The general solution of the first-order equation (32), which represents here more particularly a counter-propagating wave, is given by

$$\varepsilon(\xi_1) = \exp(2\mathrm{i}k_{\xi_1 m}\xi_1)\int_{+\infty}^{\xi_1} F(\xi)\exp(-2\mathrm{i}k_{\xi_1 m}\xi)\,\mathrm{d}\xi + C_2\exp(2\mathrm{i}k_{\xi_1 m}\xi_1), \tag{34}$$

C_2 being another arbitrary constant.

If the walls $x_3 = 0$ and $x_3 = d$ are perfectly flat (no small deformation, i.e. $\tilde{\eta}(\xi_1) = 0$ everywhere), this first-order term must vanish ($\varepsilon(\xi_1) = 0$), and then $C_1 = 0$ and $C_2 = 0$.

Finally, after integration by parts, it follows

$$\begin{aligned}\frac{\tilde{\tilde{A}}_m^{[1]}(\xi_1)}{C_m^0} = &\left[1 - \frac{\mathrm{i}}{2}k_{\xi_1 m}\varpi_m\int_0^{\xi_1}\tilde{\eta}(\xi)\,\mathrm{d}\xi\right]\exp(-\mathrm{i}k_{\xi_1 m}\xi_1)\\ &- \left[\frac{\mathrm{i}}{2}k_{\xi_1 m}\varpi_m\int_{\xi_1}^{\ell}\tilde{\eta}(\xi)\exp(-2\mathrm{i}k_{\xi_1 m}\xi)\,\mathrm{d}\xi\right]\exp(+\mathrm{i}k_{\xi_1 m}\xi_1),\end{aligned} \tag{35}$$

$\tilde{\eta}(\xi)$ vanishing for $\xi > \ell$ (ℓ denoting the total length of the corrugation). Note that this approximate result assumes that the square brackets of the last term of Eq. (35) is much smaller than one.

This result shows that the primary wave $\exp(-\mathrm{i}k_{\xi_1 m}\xi_1)$, created by the acoustic source, is slightly scattered from each point of the perturbed surface, which thus creates in the same mode secondary waves propagating, respectively, in the same direction as the primary wave and opposite (Fig. 2). This approximate approach is satisfactory when considering only one mode, but in the usual situations, inter-modal coupling must be taken into account: this is the aim of Section 4 to provide such more accurate model. Nevertheless, result (35)

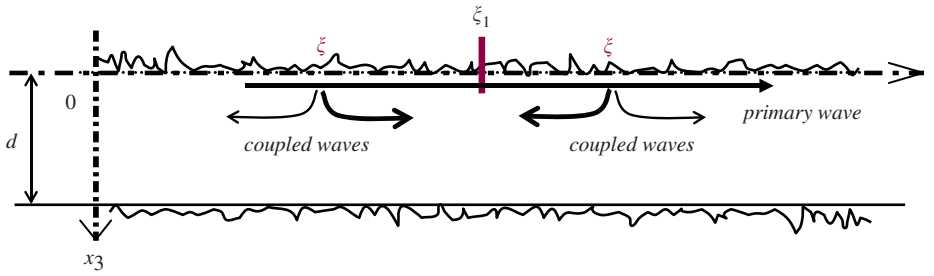

Fig. 2. Scattering phenomena of a single mode on the corrugation. The primary wave (stationary in the x_3-direction) propagates in the increasing x_1-direction while the coupled secondary waves propagate in both increasing and decreasing x_1-direction.

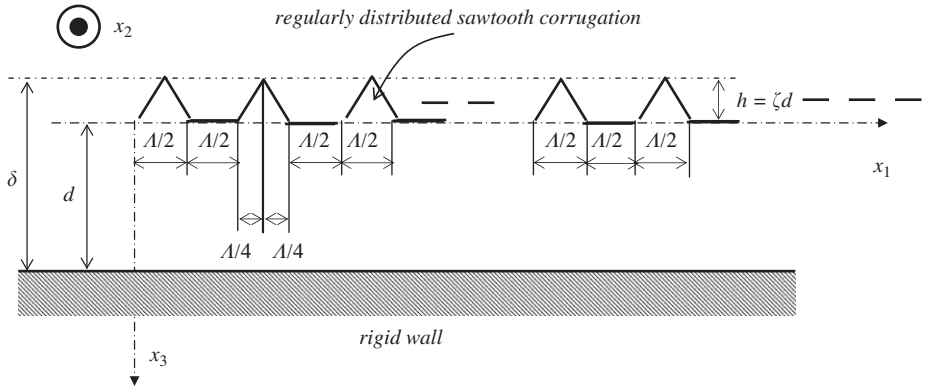

Fig. 3. Fluid plate between two rigid walls: a wall being plane and a wall having regularly distributed corrugations (sawtooth profile).

conveys interpretations of well-known physical phenomena that it is interesting to highlight here, from this very simple approach (see Section 3.3).

3.3. Phonon relation

In the case of a one-dimensional periodically corrugated surface (see an example in Fig. 3), relationships between the acoustic wavelength along the x_1-axis (or ξ_1-axis), i.e. $\lambda_{x_1 m} = 2\pi/k_{x_1 m} = 2\pi/k_{\xi_1 m}$ (see Eq. (26b)) and the length of the spatial period (denoted Λ) appear, involving a phase matching which emphasises the interference processes as shown in the following (this law of interaction between the acoustic wave and the periodic grating could be interpreted as a law of conservation of the phonon momentum in the dual space as sometimes mentioned in the literature [19]). Expanding the expression $\tilde{\eta}(\xi)$ of the periodically corrugated surface in Fourier series, the relevant point is that each sinusoidal term of the expansion contributes to the creation of secondary waves, which are represented in Eq. (35) by products of terms of the form $\exp(\pm \mathrm{i} n 2\pi/\Lambda)$ with the terms $\exp(\pm \mathrm{i} k_{x_1 m} \xi_1)$. Then, for a finite length ℓ of corrugation, the integration of the second term of the right-hand side of Eq. (35) leads to an amplitude of the secondary wave propagating backward proportional to (for the fundamental $n = 1$) $1/(2k_{x_1 m} \pm 2\pi/\Lambda)$, showing therefore a very strong coupling between the primary wave (wavenumber $k_{x_1 m}$) and the counter-propagating secondary wave (wavenumber $-k_{x_1 m}$) when satisfying the condition (phonon relation)

$$2k_{x_1 m} \pm 2\pi/\Lambda = 0. \tag{36}$$

Moreover, the integration of Eq. (35) leads also to arguments of exponential functions of the forms

$$k_{x_1 m} \quad \text{and} \quad k_{x_1 m} \pm 2\pi/\Lambda, \tag{37a}$$

which can be combined together as follows to highlight the periods appearing in the result given in Section 5:

$$\pm(2k_{x_1 m} \pm 2\pi/\Lambda)/2 \text{ and } \pi/\Lambda. \tag{37b}$$

4. Inter-modal model using approximate integral solution

The solution of problem (7) can be obtained by carrying out successive approximations of Eq. (19), using at each stage the integral formulation with an appropriate Green's function, denoted $\hat{G}_m(x_1, x_2; x_1', x_2')$.

A monochromatic source (angular frequency ω) is assumed to be flush mounted at $x_1 = 0$ and $x_2 = 0$. Its strength, related to the mth mode, is given by

$$\hat{S}_m(x_1, x_2) = \hat{Q}_m \delta(x_1)\delta(x_2), \tag{38}$$

where $\delta(x)$ is the Dirac delta function. This function $\hat{S}_m(x_1, x_2)$ vanishes for the modes, which are not created by the source, thanks to the orthogonality of the eigenfunctions considered and the source function $\hat{f}$.

Using an iterative method to express the amplitude of each mode $\hat{A}_m(x_1, x_2)$, which assumes that the coupling functions in the right-hand side of Eq. (19) are small quantities of the dimensionless parameters $\eta_0(x_1, x_2)$, $\eta_d(x_1, x_2)$ and of their derivatives with respect to the coordinates x_1 and x_2, thus the nth-order solution of Eq. (19) for $\hat{A}_m(x_1, x_2)$ is written as follows:

$$\hat{A}_m^{[n]} = \hat{A}_m^{(0)} + \hat{A}_m^{(1)} + \cdots + \hat{A}_m^{(n-1)} + \hat{A}_m^{(n)}, \tag{39}$$

where $\hat{A}_m^{[n]}$ denotes the nth-order perturbation expansion for $\hat{A}_m$, $\hat{A}_m^{(0)}$ the zero-order approximation, $\hat{A}_m^{(1)}$ the first-order correction term, and so on.

The amplitude of each mode $\hat{A}_m$ being governed by Eq. (19), the nth perturbation expansion $\hat{A}_m^{[n]}$ satisfies the approximate equation obtained by replacing $\hat{A}_m$ in the right-hand side of Eq. (19) by its expression reduced to the $(n-1)$th order.

Thus, the zero-order approximation satisfies a version of the Helmholtz equation, namely,

$$(\Delta_\parallel + k_{x_1 m}^2)\hat{A}_m^{(0)}(x_1, x_2) = -\hat{S}_m(x_1, x_2) \tag{40a}$$

and then integral formulation gives

$$\hat{A}_m^{(0)}(x_1, x_2) = \hat{Q}_m \hat{G}_m(x_1, x_2; 0, 0), \tag{40b}$$

which is the contribution of the mode m to the direct field at the receiving point x_1 when the interfaces are plane rigid walls.

Taking into account this zero-order solution and discarding the second-order terms in the right-hand side of Eq. (19), the first-order term $\hat{A}_m^{(1)}$ of the perturbation expansion is governed by Eq. (19) with $n = 1$, namely,

$$\begin{aligned}(\Delta_\parallel + k_{x_1 m}^2)[\hat{A}_m^{(0)} + \hat{A}_m^{(1)}](x_1, x_2) &= -\hat{S}_m(x_1, x_2) + \beta_{mm}\eta(x_1, x_2)(\Delta_\parallel + k_{x_1 m}^2)\hat{A}_m^{(0)}(x_1, x_2) \\ &- \sum_{\mu \neq m} N_{\mu m}(x_1, x_2)(\Delta_\parallel + k_{x_1 m}^2)\hat{A}_\mu^{(0)}(x_1, x_2) - \sum_\mu \hat{\gamma}_{\mu m}(x_1, x_2)\hat{A}_\mu^{(0)}(x_1, x_2).\end{aligned} \tag{41}$$

The expressions of $\Delta_\parallel \hat{A}_\mu^{(0)}(x_1, x_2)$ and $\Delta_\parallel \hat{A}_m^{(0)}(x_1, x_2)$ being required to satisfy Eq. (40a), this Eq. (41) gives straightforwardly

$$\begin{aligned}(\Delta_\parallel + k_{x_1 m}^2)\hat{A}_m^{(1)}(x_1, x_2) &= -\beta_{mm}\eta(x_1, x_2)\hat{S}_m(x_1, x_2) \\ &- \sum_{\mu \neq m} N_{\mu m}(x_1, x_2)\{(k_{x_1 m}^2 - k_{x_1 \mu}^2)\hat{A}_\mu^{(0)}(x_1, x_2) - \hat{S}_\mu(x_1, x_2)\} \\ &- \sum_\mu \hat{\gamma}_{\mu m}(x_1, x_2)\hat{A}_\mu^{(0)}(x_1, x_2).\end{aligned} \tag{42}$$

Then, using integral formulation with the appropriate Green's function $\hat{G}_m(x_1, x_2; x_1', x_2')$, assuming that the wall perturbation lies in the interval $0 < x_1 < \ell_1$ and $0 < x_2 < \ell_2$, and invoking expression (40b) for $\hat{A}_\mu^{(0)}(x_1, x_2)$,

leads to

$$\hat{A}_m^{(1)}(x_1,x_2)=\sum_{\mu_1}\hat{Q}_{\mu_1}\int_{+\infty}^{+\infty}\int_{+\infty}^{+\infty}\hat{G}_m(x_1,x_2;x_1',x_2')\hat{\gamma}_{\mu_1 m}(x_1',x_2')\hat{G}_{\mu_1}(x_1',x_2';0,0)\,\mathrm{d}x_1'\,\mathrm{d}x' + \sum_{\mu_1\neq m}\hat{Q}_{\mu_1}(k_{x_1 m}^2-k_{x_1\mu_1}^2)\int_{-\infty}^{+\infty}\int_{-\infty}^{+\infty}\hat{G}_m(x_1,x_2;x_1',x_2')N_{\mu_1 m}(x_1',x_2')\hat{G}_{\mu_1}(x_1',x_2';0,0)\,\mathrm{d}x_1'\,\mathrm{d}x', \quad (43)$$

and the corresponding approximate solution is

$$\hat{A}_m^{[1]}=\hat{A}_m^{(0)}+\hat{A}_m^{(1)}. \quad (44)$$

One should note that in Eq. (43) integrals from $-\infty$ to $+\infty$ are in fact integrals from 0 to ℓ_1 and ℓ_2.

When the waveguide is infinite and bounded by surfaces with one-dimensional corrugations (2D problem considered in Section 5), the coefficient of the expansion of the modal Green function is given by the one-dimensional Green's function corresponding to a point source located at a point x_1' in the waveguide is given by, for the quantum number m

$$\hat{G}_m(x_1,x_1')=\frac{\exp(-\mathrm{i}k_{x_1 m}|x_1-x_1'|)}{2\mathrm{i}k_{x_1 m}}. \quad (45)$$

Finally, the result so obtained leads straightforwardly to the following form, to the $(n+1)$th order:

$$\hat{A}_m^{[n+1]}(x_1,x_2)=\hat{A}_m^{(0)}+\sum_{\mu_1}\int_{-\infty}^{+\infty}\int_{-\infty}^{+\infty}\hat{G}_m(x_1,x_2;x_1',x_2')\hat{\gamma}_{\mu_1 m}(x_1',x_2')\hat{A}_{\mu_1}^{[n]}(x_1',x_2')\,\mathrm{d}x_1'\,\mathrm{d}x_2' - \beta_{mm}\int_{-\infty}^{+\infty}\int_{-\infty}^{+\infty}\hat{G}_m(x_1,x_2;x_1',x_2')\eta(x_1',x_2')(\Delta_\parallel+k_{x_1 m}^2)\hat{A}_m^{[n]}(x_1',x_2')\,\mathrm{d}x_1'\,\mathrm{d}x_2' + \sum_{\mu_1\neq m}\int_{-\infty}^{+\infty}\int_{-\infty}^{+\infty}\hat{G}_m(x_1,x_2;x_1',x_2')N_{\mu_1 m}(x_1',x_2')(\Delta_\parallel+k_{x_1 m}^2)\hat{A}_{\mu_1}^{[n]}(x_1',x_2')\,\mathrm{d}x_1'\,\mathrm{d}x'. \quad (46)$$

5. Results

This section aims at providing results illustrating the inter-modal model using periodically or "quasi-random" one-dimensional corrugated surfaces (2D problem). The phonon relationships, which are written in Section 3.3 for the monomode approach are first extended in Section 5.1, which permits to highlight strong couplings between modes in the vicinity of these phonon relationships for periodically corrugated surfaces. The last Section 5.2 focuses mainly on the propagation upstream and downstream the corrugated domain for periodic or "quasi-random" sawtooth profiles.

5.1. Influence of a phonon relationship

As already mentioned in Section 3.3, relationships between the length of the spatial period (denoted Λ) and the acoustic wavelengths along the x_1-axis ($\lambda_{x_1 m}=2\pi/k_{x_1 m}$ for the mode m generated by the source and $\lambda_{x_1\mu}=2\pi/k_{x_1\mu}$ for the modes μ created by the scattering on the corrugation) appear, involving a phase matching which emphasises the interference processes (phonon relations [19]), namely,

$$k_{x_1 m}+k_{x_1\mu}\pm 2\pi/\Lambda=0, \quad (47a)$$

i.e. using Eq. (20d),

$$\frac{k_{x_1\mu}d}{2\pi}=\pm\frac{d}{\Lambda}-\sqrt{\left(\frac{fd}{c_0}\right)^2-\left(\frac{m}{2}\right)^2} \quad (47b)$$

and showing therefore a strong coupling between the primary wave (wavenumber $k_{x_1 m}$) and the counter-propagating secondary wave (wavenumber $-k_{x_1\mu}$). The intersection in the plane (fd/c_0, $k_{x_1 m}d/(2\pi)$) of the

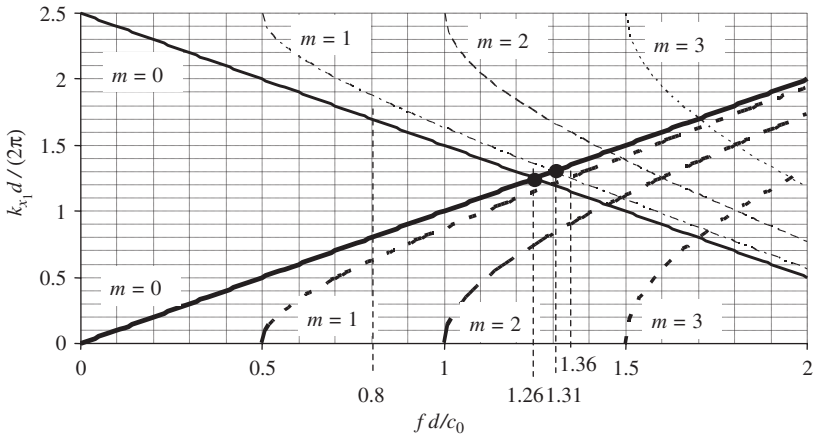

Fig. 4. Dispersion curves (thick lines) of the guide with smooth interfaces ($k_{x_1} d/(2\pi) = \sqrt{(fd/c_0)^2 - (m/2)^2}$), and curves (thin lines) corresponding to the phonon relation (47) ($k_{x_1} d/(2\pi) = d/\Lambda - \sqrt{(fd/c_0)^2 - (m/2)^2}$). Solid lines: mode $m = 0$, dash–dot lines: mode $m = 1$, dashed lines: $m = 2$, dotted lines: $m = 3$.

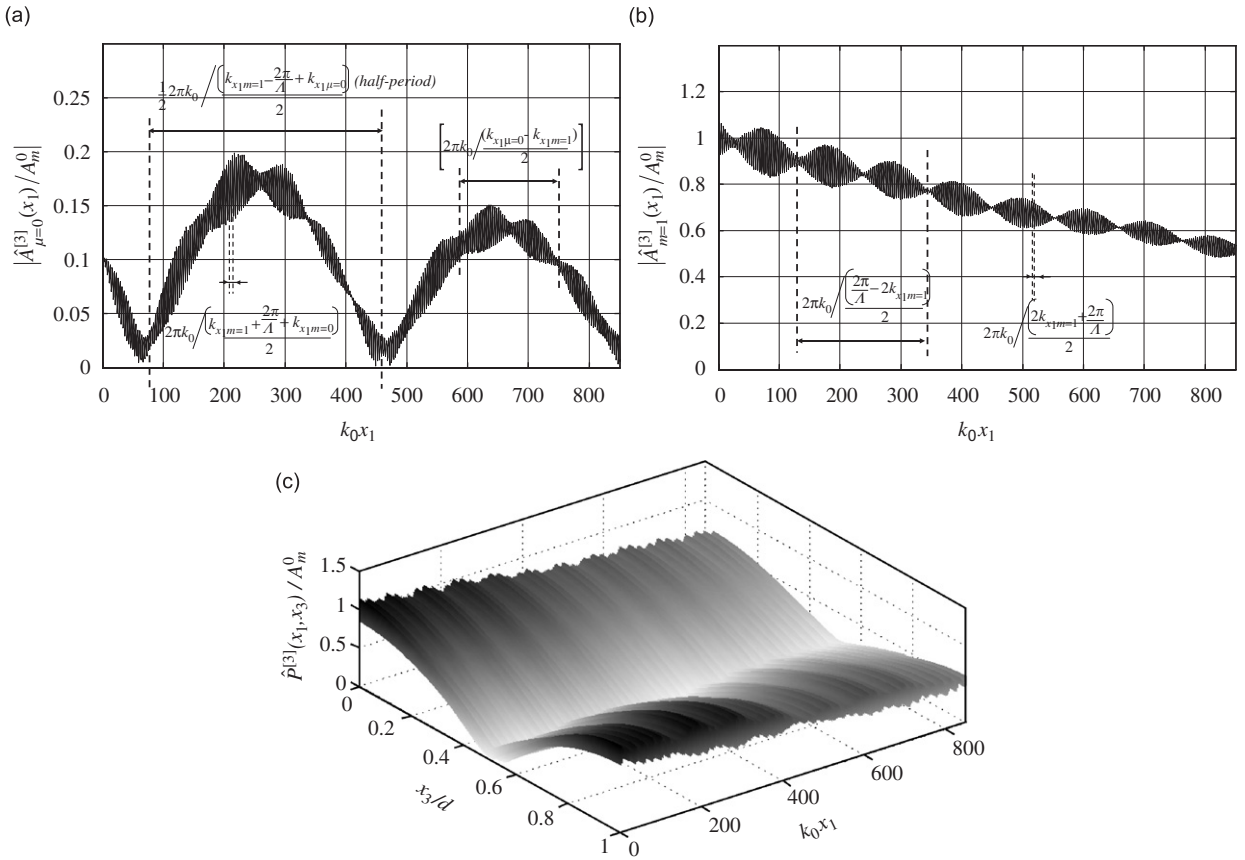

Fig. 5. Modulus of the normalised amplitude of the pressure variation (third order) for a sawtooth profile (see Fig. 3): (a) $\hat{A}^{[3]}_{\mu=0}(x_1)/A^0_m$ for the mode $\mu = 0$, (b) $\hat{A}^{[3]}_{m=1}(x_1)/A^0_m$ of the mode $m = 1$ (the only mode generated by the source) and (c) $|\hat{P}^{[3]}(x_1)/A^0_m|$ of the total pressure variation, when $f_d/c_0 = 1.31$ and $d/\Lambda = 2.5$. The length ℓ of the corrugation at $x_3 = 0$ is such as $k_0\ell = 867.5$ ($\ell \approx 138.1\lambda$) which corresponds to $N = 264$ teeth (see Table 1 for dimensional quantities). The heights of the teeth are such as $\zeta = 0.005$; the interface $x_3 = d$ is smooth.

dispersion curves (thick lines in Fig. 4) with the curves (thin lines in Fig. 4 for $d/\Lambda = 2.5$) representing the phonon relation (Eq. (47b) with $+d/\Lambda$), permits to predict the values of the frequencies for which there could exist such a strong coupling for a given ratio d/Λ.

As an example, for $fd/c_0 \approx 1.31$, the thin line which represents the phonon relation (47b) for $m = 1$ has an intersection with the dispersion curve of the regular-shaped guide corresponding to $\mu = 0$ (labelled $m = 0$ in Fig. 4). Therefore, when the source creates the mode $m = 1$, a strong coupling appears with the coupled mode $\mu = 0$. Moreover, as there is an intersection of this thin line with the dispersion curve of the guide for the mode $m = 1$ at a value of $fd/c_0 \approx 1.36$ (thus closed to 1.31), a strong self-coupling between the mode $m = 1$ created by the source and the same mode $\mu = 1$ appears, perturbing this mode $m = 1$.

This phenomenon is illustrated on the particular case of a periodically sawtooth profile (shown in Fig. 3) assumed to be of infinite extent. The acoustic source is assumed to create only the mode $m = 1$ (incoming wave), at the forcing frequency f. Four modes are considered in the solution: for the chosen frequency ($fd/c_0 \approx 1.31$ with $d/\Lambda = 2.5$), the first three modes ($\mu = 0, 1, 2$) are propagative and the last one ($\mu = 3$) is evanescent. The chosen frequency is in the vicinity of the value given by the phonon relation (47b), thus both a strong coupling between the mode $m = 1$ created by the source and the coupled mode $\mu = 0$, and a quite strong "self-coupling" of the mode $m = 1$ occur, as it can be seen in Figs. 5a and b, which present the modulus of the normalised amplitudes of the modes 0 and 1 as a function of the dimensionless parameter $k_0 x_1$ (propagative mode $\mu = 2$ and evanescent mode $\mu = 3$ are not represented: their amplitudes vanish because their coupling with the other modes are very weak). Fig. 5c shows the total normalised pressure variation which results from the superposition of the modes $m = 0, 1, 2, 3$ (Eq. (14)).

As explained in Section 3.3, expanding the expression $\eta(x_1)$ of the periodically corrugated surface in Fourier series leads to arguments of exponential functions of the forms

$$k_{x_1 m}, k_{x_1 \mu}, k_{x_1 m} \pm 2\pi/\Lambda \quad \text{and} \quad k_{x_1 m} + k_{x_1 \mu} \pm 2\pi/\Lambda, \tag{48a}$$

Table 1
Characteristics of two media, a fluid one (air) and a fluid-like one (glass with only longitudinal waves), and characteristics of the corrugation for each one, as a function of the dimensionless parameters fd/c_0 and d/Λ: $k_0 = (2\pi/d)(fd/c_0)$; $\lambda = d/(fd/c_0)$; $f = (c_0/d)(fd/c_0)$; $\Lambda/\lambda = (fd/c_0)/(d/\Lambda)$ and $\ell = (2N-1)\Lambda/2$

			Air	"Glass" (for longitudinal waves)
		c_0 (m s^{-1})	340	5825
		ρ_0 (kg m^{-3})	1.2	5000
		d (m)	5	0.005
$fd/c_0 = 1.31$		λ (m)	3.8	0.0038
$d/\Lambda = 2.5$		Λ/λ	0.524	0.524
		f (kHz)	0.089	1526
		k_0 (m^{-1})	1.646	1646
	$k_0\ell = 261.7$; $N = 80$	ℓ (m)	159	0.159
	$k_0\ell = 867.5$; $N = 264$	ℓ (m)	527	0.527
$fd/c_0 = 1.26$		λ (m)	3.97	0.00397
$d/\Lambda = 2.5$		Λ/λ	0.504	0.504
		f (kHz)	0.0857	1468
		k_0 (m^{-1})	1.583	1583
	$k_0\ell = 207.4$; $N = 66$	ℓ (m)	131	0.131
$fd/c_0 = 0.80$		ℓ (m)	6.25	0.00625
$d/\Lambda = 2.5$		Λ/λ	0.32	0.32
		f (kHz)	0.0544	932
		k_0 (m^{-1})	1.005	1005
	$k_0\ell = 131.7$; $N = 66$	ℓ (m)	131	0.131
	$k_0\ell = 529.8$; $N = 264$	ℓ (m)	527	0.527

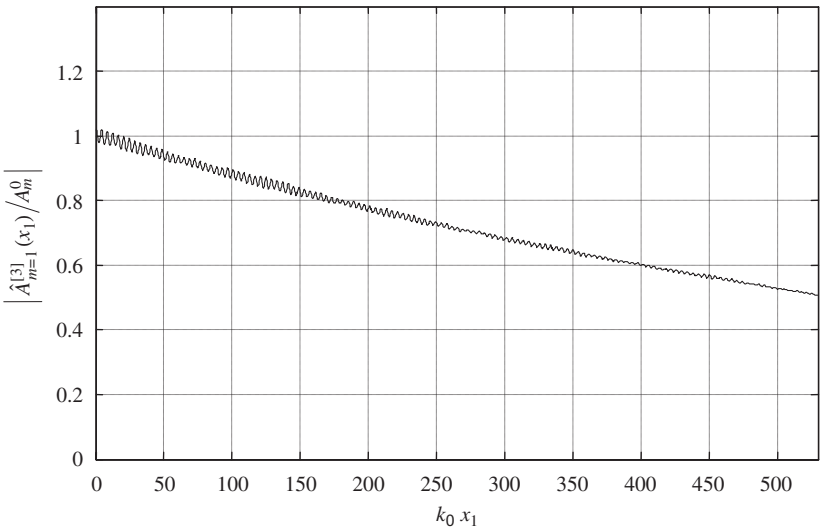

Fig. 6. Modulus of the normalised amplitude of the pressure variation (third order) for a sawtooth profile (see Fig. 3) $\hat{A}^{[3]}_{m=1}(x_1)/A^0_m$ for the mode $m=1$ (the only mode generated by the source), when $fd/c_0=0.8$ and $d/\Lambda=2.5$. The length ℓ of the corrugation at $x_3=0$ is such as $k_0\ell=529.8$ ($\ell\approx 84.32\lambda$) which corresponds to $N=264$ teeth (see Table 1 for dimensional quantities). The heights of the teeth are such as $\zeta=0.005$; the interface $x_3=d$ is smooth.

Table 2
Cut-off frequencies of the two fluid-like media of Table 1, for the first four modes

	$m=0$	$m=1$	$m=2$	$m=3$
Air (Hz)	0	34	68	102
"Glass" (for longitudinal waves) (MHz)	0	0.5825	1.165	1.748

which can be combined together as follows to highlight the periods appearing in Figs. 5a and b in the result given below:

$$\frac{1}{2}\left(k_{x_1 m}\pm\frac{2\pi}{\Lambda}+\left\{\begin{array}{c}+k_{x_1\mu}\\ -k_{x_1\mu}\\ +2k_{x_1\mu}\end{array}\right\}\right)\quad\text{and}\quad\frac{1}{2}(k_{x_1 m}-k_{x_1\mu}). \tag{48b}$$

Finally, it can be observed in Figs. 5a and b that the amplitude of the modes $m=1$ and $\mu=0$ decrease when the abscissa of the observation point (k_0x_1) increases. For the mode $m=1$ (Fig. 5b), this decrease has an approximate exponential shape, with an attenuation factor equal to approximately $10^{-3}\,\mathrm{mm}^{-1}$ for the "glass" plate (Table 1). This value has the same order of magnitude ($1.5\times10^{-3}\,\mathrm{mm}^{-1}$) as that experimentally found in solid media for roughness profile (shot blasted plate), when A_1 Lamb mode propagates [21,22].

The same phenomenon can be observed in Fig. 6, which presents the same result as for Fig. 5b except that the frequency ($fd/c_0=0.8$ with $d/\Lambda=2.5$) does not satisfy the phonon relation (48b) as one can see in Fig. 4. Here, the amplitude of the oscillations is much lower, showing that the self-coupling of the mode $m=1$ is weak.

Nota Bene: In order to clarify the orders of magnitude, the dimensional different quantities of interest (frequencies, wavelengths, etc.) are listed in Table 1 for two fluid-type media: the air (a real fluid) and the glass when (only the longitudinal waves are taken into account) (Table 2).

5.2. Propagation upstream and downstream a corrugated domain of finite extent

This section aims at going further in the interpretation of the results and at focusing mainly on the propagation upstream and downstream the perturbed domain (corrugation).

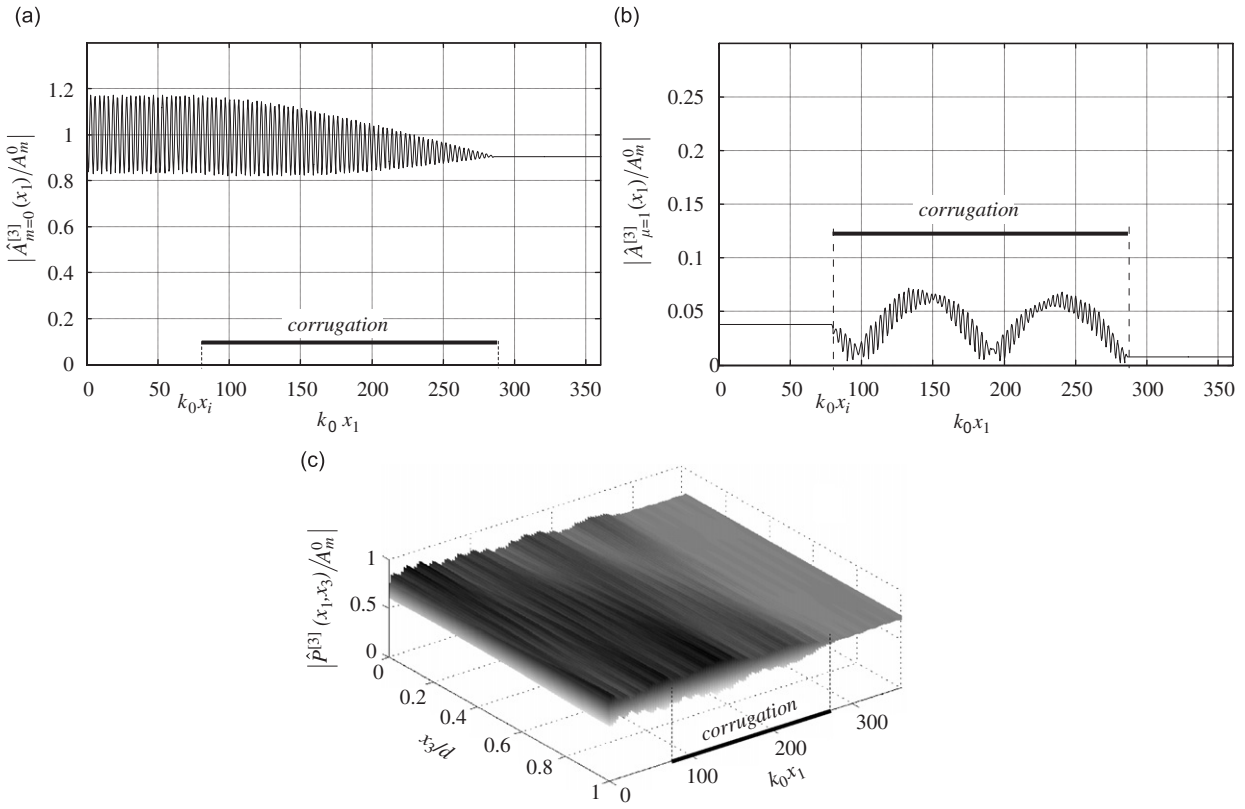

Fig. 7. Modulus of the normalised amplitude of the pressure variation (third order) for a sawtooth profile (see Fig. 3): (a) $\hat{A}^{[3]}_{m=0}(x_1)/A^0_m$ for the mode $m=0$ (the only mode generated by the source), (b) $\hat{A}^{[3]}_{\mu=1}(x_1)/A^0_m$ for the mode $\mu=1$ and (c) $|\hat{P}^{[3]}(x_1)/A^0_m|$ of the total pressure variation, when $fd/c_0 = 1.26$ and $d/\Lambda = 2.5$. The coordinates of the ends of the corrugation are x_i and $(x_i+\ell)$ with $k_0 x_i = 79.2$, the length ℓ of the corrugation at $x_3 = 0$ being such as $k_0\ell = 207.4$ ($\ell \approx 33\lambda$) which corresponds to $N = 66$ teeth (see Table 1 for dimensional quantities). The heights of the teeth are such as $\zeta = 0.005$; the interface $x_3 = d$ is smooth.

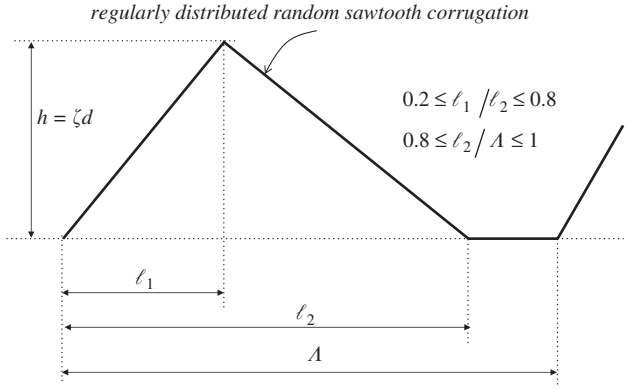

Fig. 8. Random sawtooth profile. The spatial wavelength Λ is a constant, but the height of the teeth and the ratios ℓ_1/ℓ_2 and ℓ_2/Λ are random.

It is assumed that, inside the 2D waveguides bounded by two parallel plates which are considered below, the only mode created by the source is the mode $m = 0$ and that the frequency is such as $fd/c_0 = 1.26$ with $d/\Lambda = 2.5$, so as a phonon relation is satisfied (thus a strong "self-coupling" of the mode $m = 0$ and a quite strong coupling with the coupled mode $\mu = 1$ occur, see Fig. 4). The corrugations start at the "input" abscissa x_i such as $k_0 x_i \approx 80$, and the length ℓ of the corrugations are such as $k_0\ell = 207.4$ which corresponds to $N = 66$ teeth (see Table 1 for dimensional quantities) and to $\ell \approx 33\lambda$ for the fluid-like media indicated in Table 1. The heights $h = \zeta d$ of the teeth are such as $\zeta = 0.005$.

Four sets of results are shown, corresponding to four different sawtooth profiles. The modulus of the normalised amplitudes of the modes considered and the corresponding total acoustic pressure, as functions of the observation point, are shown in Figs. 7a–c, 9a, b, 11a, b and 12a–c, respectively, for a periodic sawtooth

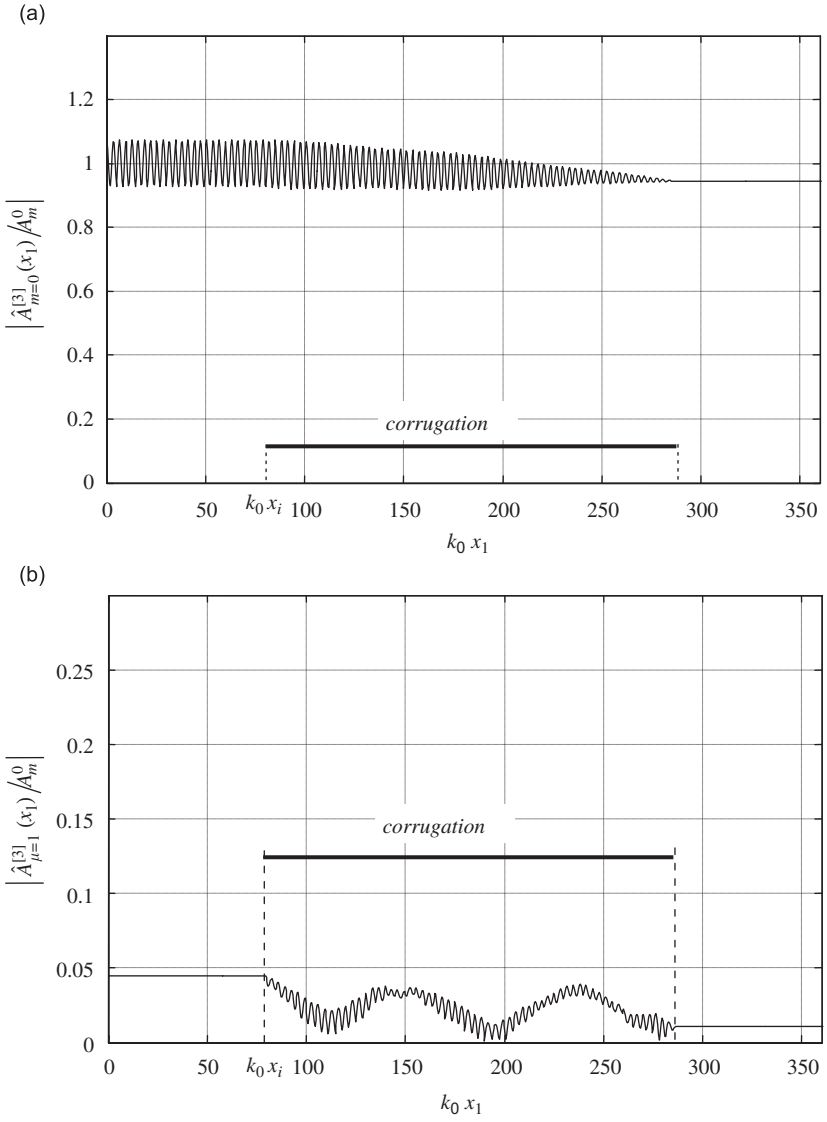

Fig. 9. Modulus of the normalised amplitude of the pressure variation (third order) a random sawtooth profile (see Fig. 8): (a) $\hat{A}^{[3]}_{m=0}(x_1)/A^0_m$ for the mode $m = 0$ (the only mode generated by the source), (b) $\hat{A}^{[3]}_{\mu=1}(x_1)/A^0_m$ for the mode $\mu = 1$, when $fd/c_0 = 1.26$ and $d/\Lambda = 2.5$. The coordinates of the ends of the corrugation are x_i and $(x_i + \ell)$ with $k_0 x_i = 79.2$, the length ℓ of the corrugation at $x_3 = 0$ being such as $k_0\ell = 207.4$ ($\ell \approx 33\lambda$) which corresponds to $N = 66$ teeth (see Table 1 for dimensional quantities). The heights of the teeth are such as the nondimensional parameter ζ is contained between 0.0015 and 0.005; the interface $x_3 = d$ is smooth.

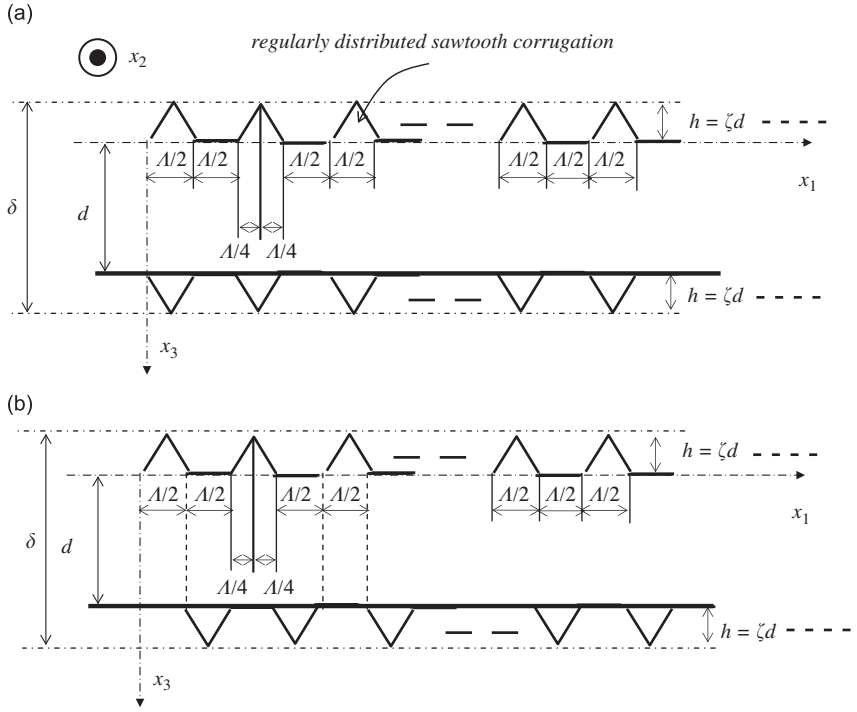

Fig. 10. Regularly distributed sawtooth profile on each side of the plate: (a) in phase symmetric profile and (b) out of phase symmetric profile.

profile at the interface $x_3 = 0$ (Fig. 3), "quasi-random" profile (Fig. 8), the same periodic sawtooth profile on each side of the waveguide ($x_3 = 0$ and d), symmetrically (Fig. 10a) or antisymmetrically (Fig. 10b) corrugated.

For each case, the backward propagation (Figs. 7a, 9a, 11a and 12a), already highlighted by Eq. (35) in the mono-mode approach (see Section 3.3 and Fig. 3) and created by the back-scattering on corrugation, is obvious upstream the corrugation ($x_1 < x_i$), showing interferences between the incident wave and the counter-propagating wave. Downstream the corrugation, the mean level of the incident mode depends on the profile because the mode created by the source decreases when the abscissa of the observation point increases.

For the coupled mode $\mu = 1$ (Figs. 7b, 9b and 12b), oscillations occur only inside the corrugation as expected.

When the sawtooth profile is randomly distributed [i.e. when each tooth has a triangular profile, the lengths ℓ_1 and ℓ_2 (see Fig. 8) being distributed randomly with $0.2 \leqslant \ell_1/\ell_2 \leqslant 0.8$ and the both being distributed regularly with a spatial period Λ ($0.8 \leqslant \ell_2/\Lambda \leqslant 1$)], the general shapes of the curves shown in Figs. 9a and b are the same as those given in Figs. 7a and b for a periodic sawtooth profile with the same spatial wavelength Λ, but the amplitude of the modes are lower due to the random character of the profile.

On the other hand, for a symmetrically corrugated (sawtooth profile) waveguide (Fig. 10a), the amplitudes of both the modes such as $(m+\mu)$ are even numbers and the total pressure (Fig. 11a for $m = \mu = 0$ and Fig. 11b, respectively) are greater than the amplitudes obtained when the interface $x_3 = d$ is smooth (Figs. 7a and c), whereas the amplitude of the modes such as $(m+\mu)$ are odd numbers vanishes. These results can be explained from expressions (18b) and (13a) of the coupling factors $\alpha_{\mu m}^{(j)} \partial_{x_j}$ and $k_m^2 B_{\mu m}$, invoking the expression (13b) of $\beta_{\mu m}$: for this symmetrical profile, the normalised depths η_0 and η_d are equal (Eq. (11)), and thus the coupling factors double in amplitude when $(m+\mu)$ are even numbers and vanish when $(m+\mu)$ are odd numbers. For antisymmetrical sawtooth profile (Fig. 10b), this kind of properties does not appear anymore (Figs. 12a–c).

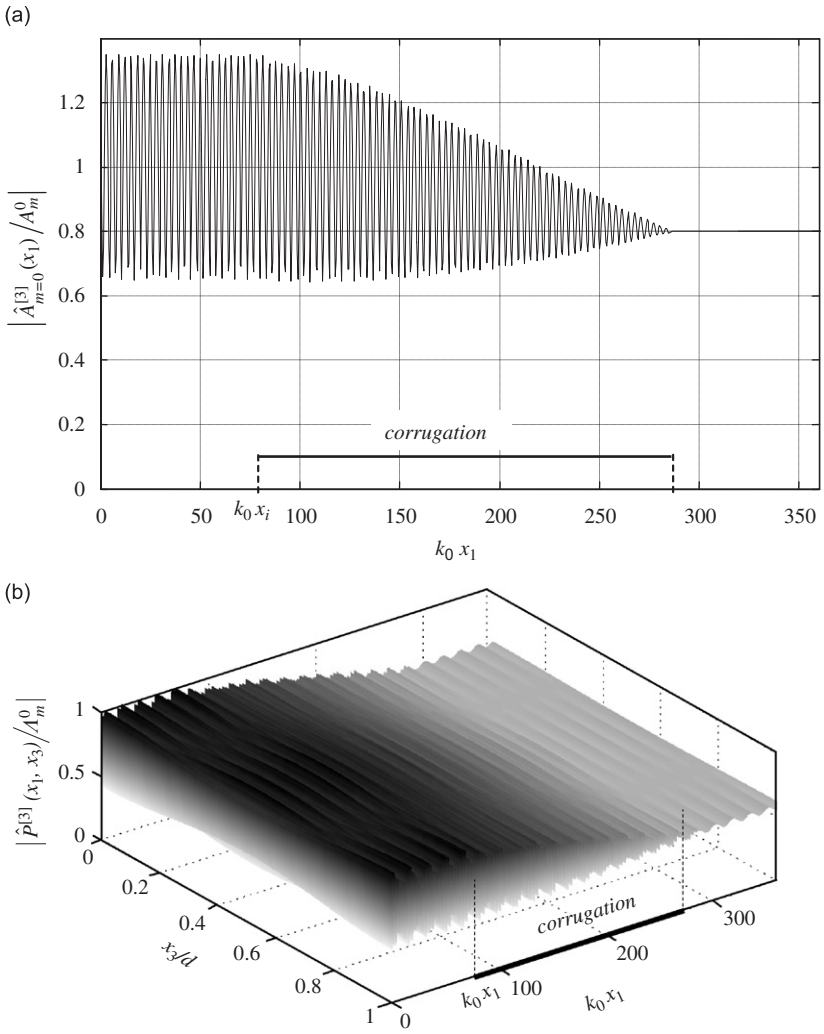

Fig. 11. Modulus of the normalised amplitude of the pressure variation (third order) for a sawtooth profile on each side of the plate (see Fig. 10a): (a) $\hat{A}^{[3]}_{m=0}(x_1)/A^0_m$ for the mode $m=0$ (the only mode generated by the source) and (b) $|\hat{P}^{[3]}(x_1)/A^0_m|$ of the total pressure variation, when $fd/c_0 = 1.26$ and $d/\Lambda = 2.5$. The coordinates of the ends of the corrugation are x_i and $(x_i+\ell)$ with $k_0 x_i = 79.2$, the length ℓ of the corrugation at $x_3 = 0$ being such as $k_0\ell = 207.4$ ($\ell \approx 33\lambda$) which corresponds to $N = 66$ teeth (see Table 1 for dimensional quantities). The heights of the teeth are such as $\zeta = 0.005$.

6. Conclusion

The general subject matter of the paper is the modelling of the inter-modal couplings in waveguides with nonhomogeneously shaped walls, the shape (the slope) and the depth of the perturbed surfaces being both taken into account, assuming Neumann conditions (shape profile model).

A mono-mode approximation which consists in considering only one acoustic mode by neglecting the coupling between different modes, leads to a simple interpretation of the involved physical phenomena: the couplings due to the scattering from the perturbed surface distribute the acoustic energy in the same mode than the one first considered (created by the acoustic source), through secondary waves propagating, respectively, in the same direction as the primary wave or opposite, and phonon relations can be highlighted.

In the inter-modal couplings approach, the continuously distributed modes coupling along the distributed slight geometrical perturbation are accounted for in using method relying on integral formulation and modal analysis.

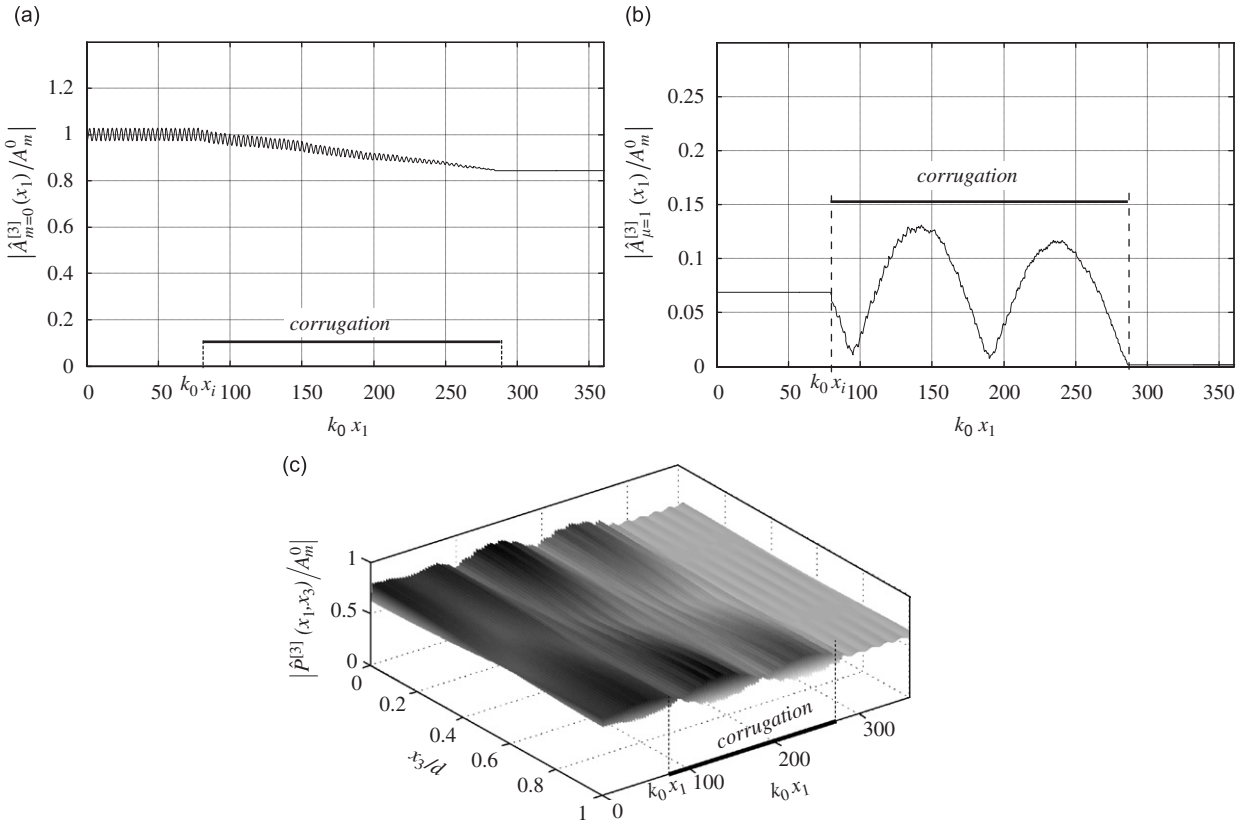

Fig. 12. Modulus of the normalised amplitude of the pressure variation (third order) for a sawtooth profile on each side of the plate (see Fig. 10b): (a) $\hat{A}^{[3]}_{m=0}(x_1)/A^0_m$ for the mode $m=0$ (the only mode generated by the source) and (c) $|\hat{P}^{[3]}(x_1)/A^0_m|$ of the total pressure variation, when $fd/c_0 = 1.26$ and $d/\Lambda = 2.5$. The coordinates of the ends of the corrugation are x_i and $(x_i+\ell)$ with $k_0 x_i = 79.2$, the length ℓ of the corrugation at $x_3 = 0$ being such as $k_0\ell = 207.4$ ($\ell \approx 33\lambda$) which corresponds to $N = 66$ teeth (see Table 1 for dimensional quantities). The heights of the teeth are such as $\zeta = 0.005$.

The numerical results analysed in Section 5 highlight the following points, showing that the shape profile model is successful in several simple situations but also that it can handle a variety of more realistic situations:

(i) Phonon relations are highlighted by the oscillations of the amplitudes of the modes having specific spatial periods, showing the strong couplings between modes.
(ii) When a phonon relation is not approximately (or exactly) verified, the global shape of the amplitude as function of the observation point is the same, but the amplitude of the oscillations are smaller than those obtained when the phonon relation is verified.
(iii) The amplitude of the modes created by the acoustic source decreases when the abscissa of the observation point increases along the corrugation, as expected when comparing with experimental results obtained in isotropic solid media.
(iv) The backward propagation is emphasised by the presence, upstream the corrugation region, of modes created by the scattering on the corrugation.
(v) When the guide, bounded by two planes, is corrugated on each side with symmetrical profiles, the odd or even character of the quantum number modes provides an increase (compared with the case of only one corrugated interface) or a cancellation of the coupling.
(vi) A "quasi-random" periodic profile just leads to a diminution of the oscillation amplitudes of the modes, compared with a regular periodic profile.

It can be emphasised that the examples presented here have highlighted the feasibility of the method in having given results, which assume Neumann boundary conditions. Given the specificity of these examples, it is clear that the Dirichlet problems, even problems with mixed boundary conditions, are similar analytic problems to the Neumann one, in the framework of this paper, thereby supporting the methods for applications involving compressional waves in fluid or solid waveguides with nonhomogeneously shaped walls.

Acknowledgements

Support from CNRS through the research group (GDR-2501) is gratefully acknowledged. The authors wish to thank their colleagues in this group for valuable discussions. The authors also want to thank the reviewers for helpful suggestions.

Appendix A. Expressions of the function $N_{\mu m}(x_1, x_2)$ (Section 2.3, Eq. (10))

The integral

$$N_{\mu m}(x_1, x_2) = \int_{H_0}^{\delta - H_d} \psi_m(x_3)\psi_\mu(x_3)\,\mathrm{d}x_3 \tag{A.1}$$

takes various forms, depending on the values of the quantum numbers m and μ.

When $m = \mu$,

$$N_{mm}(x_1, x_2) = -\frac{(1-\delta_{m0})}{2m\pi}\{\sin(2m\pi\eta_d) + \sin(2m\pi\eta_0)\} + 1 - \eta(x_1, x_2), \tag{A.2}$$

where

$$\eta(x_1, x_2) = \eta_0(x_1, x_2) + \eta_d(x_1, x_2), \tag{A.3a}$$

$$\eta_0(x_1, x_2) = H_0(x_1, x_2)/\delta, \tag{A.3b}$$

$$\eta_d(x_1, x_2) = H_d(x_1, x_2)/\delta \tag{A.3c}$$

and when $m \neq \mu$,

$$\frac{2N_{\mu m}(x_1, x_2)}{\sqrt{(2-\delta_{m0})(2-\delta_{\mu 0})}} = \frac{1}{(m+\mu)\pi}\{(-1)^{m+\mu}\sin[-(m+\mu)\pi\eta_d] + \sin[-(m+\mu)\pi\eta_0]\} + \frac{1}{(m-\mu)\pi}\{(-1)^{m-\mu}\sin[-(m-\mu)\pi\eta_d] + \sin[-(m-\mu)\pi\eta_0]\}. \tag{A.4}$$

References

[1] P.M. Morse, H. Feshbach, *Methods of Theoretical Physics—part II*, McGraw-Hill, New York, 1953, pp. 999–1064.
[2] I.J. Cooper, H.F. Pollard, Low frequency resonances in unsymmetrical enclosures, *Acustica* 41 (1978) 86–93.
[3] P. Herzog, M. Bruneau, Shape perturbation and inertial mode coupling in cavities, *Journal of the Acoustical Society of America* 86 (1989) 2377–2384.
[4] P. Hamery, P. Dupire, M. Bruneau, Acoustic fields in trapezoidal cavities, *Acustica United with Acta Acustica* 83 (1997) 13–18.
[5] J. Missaoui, L. Cheng, A combined integro-modal approach for predicting acoustic properties of irregular-shaped cavities, *Journal of the Acoustical Society of America* 101 (1997) 3313–3321.
[6] Y.Y. Li, L. Cheng, Modifications of acoustic modes and coupling due to a leaning wall in a rectangular cavity, *Journal of the Acoustical Society of America* 116 (2004) 3312–3318.
[7] K.S. Sum, J. Pan, Effects of the inclination of a rigid wall on the free vibration characteristics of acoustic modes in a trapezoidal cavity, *Journal of the Acoustical Society of America* 119 (2006) 2201–2210.
[8] J.B. Mehl, M.R. Moldover, L. Pitre, Designing quasi-spherical resonators for acoustic thermometry, *Metrologia* 41 (2004) 295–304.

[9] B. Sapoval, O. Haeberle, S. Russ, Acoustical properties of irregular and fractal cavities, *Journal of the Acoustical Society of America* 102 (1997) 2014–2019.
[10] M. Bruneau, T. Scelo (translator and contributor), *Fundamentals of Acoustics*, ISTE, UK, USA, 2006.
[11] N. Sugimoto, M. Masuda, T. Hashiguchi, Frequency response of nonlinear oscillations of air column in a tube with an array of Helmholtz resonators, *Journal of Acoustical Society of America* 114 (2003) 1772–1784.
[12] S. Banerjee, T. Kundu, Elastic wave propagation in sinusoidally corrugated waveguides, *Journal of the Acoustical Society of America* 119 (2006) 2006–2017.
[13] D.H. Berman, Reverberation in waveguides with rough surfaces, *Journal of the Acoustical Society of America* 105 (1999) 672–686.
[14] D.E. Chimenti, O.I. Lobkis, The effect of rough surfaces on guided waves in plates, *Ultrasonics* 36 (1998) 155–162.
[15] B.I. Boyanof, V.L. Strashilov, Transmission and reflection coefficients for surface transverse waves propagating under shorted metal strip gratings, *IEEE Transactions on Ultrasonics, Ferroelectrics, and Frequency Control* 39 (1992) 119–121.
[16] M.A. Hawwa, Acoustic/elastic stop-band interaction in waveguides involving two periodicities, *Journal of the Acoustical Society of America* 102 (1997) 137–142.
[17] D.H. Berman, Effective reflection coefficients for the mean acoustic field between two rough interfaces, *Journal of the Acoustical Society of America* 96 (1994) 417–426.
[18] O.I. Lobkis, D.E. Chimenti, Elastic guided waves in plates with surface roughness. I. Model calculation, *Journal of the Acoustical Society of America* 102 (1997) 143–149.
[19] D. Leduc, A.-C. Hladky, B. Morvan, J.-L. Izbicki, P. Pareige, Propagation of Lamb waves in a plate with a periodic grating: interpretation by phonon, *Journal of the Acoustical Society of America* 118 (2005) 2234–2239.
[20] V. Pagneux, A. Morel, Lamb wave propagation in elastic waveguides with variable thickness, *Proceedings of the Royal Society A: Mathematical, Physical and Engineering Sciences* 462 (2006) 1315–1339.
[21] C. Potel, D. Leduc, B. Morvan, P. Pareige, J.L. Izbicki, C. Depollier, Lamb wave propagation in isotropic media with rough interface: comparison between theoretical and experimental results, *Fifth World Congress on Ultrasonics*, Collected Papers on CD-ROM ISBN 2-9521105-0-6, Paris, France, 2003, pp. 609–612.
[22] C. Potel, D. Leduc, B. Morvan, P. Pareige, C. Depollier, J.L. Izbicki, Propagation of Lamb waves in anisotropic rough plates: a perturbation method, *Proceedings of the Joint Congress CFA/DAGA'047*, Collected Papers on CD-ROM ISBN 2-9521105-3-0, Strasbourg, 2004, pp. 147–148.
[23] A. Boström, Propagating, damped, and leaky surface waves on the corrugated traction-free boundary of an elastic half-space, *Journal of the Acoustical Society of America* 85 (1989) 1549–1555.
[24] A. El-Bahrawy, Stopbands and passbands for symmetric Rayleigh–Lamb modes in a plate with corrugated surfaces, *Journal of Sound and Vibration* 170 (1994) 145–160.
[25] N.F. Declercq, J. Degrieck, R. Briers, O. Leroy, Diffraction of homogeneous and inhomogeneous plane waves on a doubly corrugated liquid/solid interface, *Ultrasonics* 43 (2005) 605–618.
[26] T. Kundu, S. Banerjee, K.V. Jata, An experimental investigation of guided wave propagation in corrugated plates showing stop bands and pass bands, *Journal of the Acoustical Society of America* 120 (2006) 1217–1226.
[27] S. Banerjee, T. Kundu, Symmetric and anti-symmetric Rayleigh–Lamb modes in sinusoidally corrugated waveguides: an analytical approach, *International Journal of Solids and Structures* 43 (2006) 6551–6567.
[28] Y.Y. Lu, J. Huang, J. McLaughlin, Local orthogonal transformation and one-way methods for acoustic waveguides, *Wave Motion* 34 (2001) 193–207.
[29] B. Nilsson, Acoustic transmission in curved ducts with varying cross-sections, *Proceedings of the Royal Society A: Mathematical, Physical and Engineering Sciences* 458 (2002) 1555–1574.